We are IntechOpen, the world's leading publisher of Open Access books
Built by scientists, for scientists

4,800
Open access books available

122,000
International authors and editors

135M
Downloads

Our authors are among the

154
Countries delivered to

TOP 1%
most cited scientists

12.2%
Contributors from top 500 universities

CLARIVATE ANALYTICS
BOOK CITATION INDEX
INDEXED

WEB OF SCIENCE™

Selection of our books indexed in the Book Citation Index
in Web of Science™ Core Collection (BKCI)

Interested in publishing with us?
Contact book.department@intechopen.com

Numbers displayed above are based on latest data collected.
For more information visit www.intechopen.com

Chapter

Ionospheric Monitoring and Modeling Applicable to Coastal and Marine Environments

Ljiljana R. Cander and Bruno Zolesi

Abstract

Ionospheric monitoring and modeling in costal and marine environment is reviewed and characterized in terms of state of art, global, regional, and local issues across different domains of solar-terrestrial conditions for practical applications. Their effects on critical technological systems are either controlled by the Earth's ionosphere, as in telecommunications and information systems, or simply influenced by its variability, as in trans-ionospheric radio communication, and navigation systems. The evolution of long-distance high-frequency (HF) communications and then still the actuality of HF radio links especially for the coast environment, maritime services, and aeronautical applications, for control and emergency services, for communications equally important in case of great islands and remote areas, for economic reasoning and easy management, and for efficient backup in case of cyber threats are discussed. Some preferred methods for a proper assessment of HF networks have been identified, and examples of existing long-term prediction and near real-time nowcasting in ionospheric space weather modeling to be used, particularly in the Mediterranean area, are presented along with contemporary references.

Keywords: ionosphere, space weather, model, HF and GNSS systems

1. Introduction

Variability in the Earth's ionosphere reduces the reliability of radio-frequency (RF) and global navigation satellite system (GNSS) communication systems because they depend on the attenuation, absorption, reflection, and refraction and accordingly changes in the propagation, phase, and amplitude characteristics of radio waves, in addition to the scintillation phenomenon induced by abrupt variations in electron density along the radio path. Significant scientific work over many decades, within national and international projects, is being conducted on monitoring, proper understanding, and predicting ionospheric variability in order to enhance reliability and robustness of both ground- and space-based communications networks and other applications for the benefit of society [1].

Ionospheric bottom- and topside observations and studies related to fundamental as well as radio communication and navigation purposes cover most of the planet but in an inhomogeneous way. Accordingly, the discovery and complete characterization phase for most ionospheric processes is still in progress. This is particularly
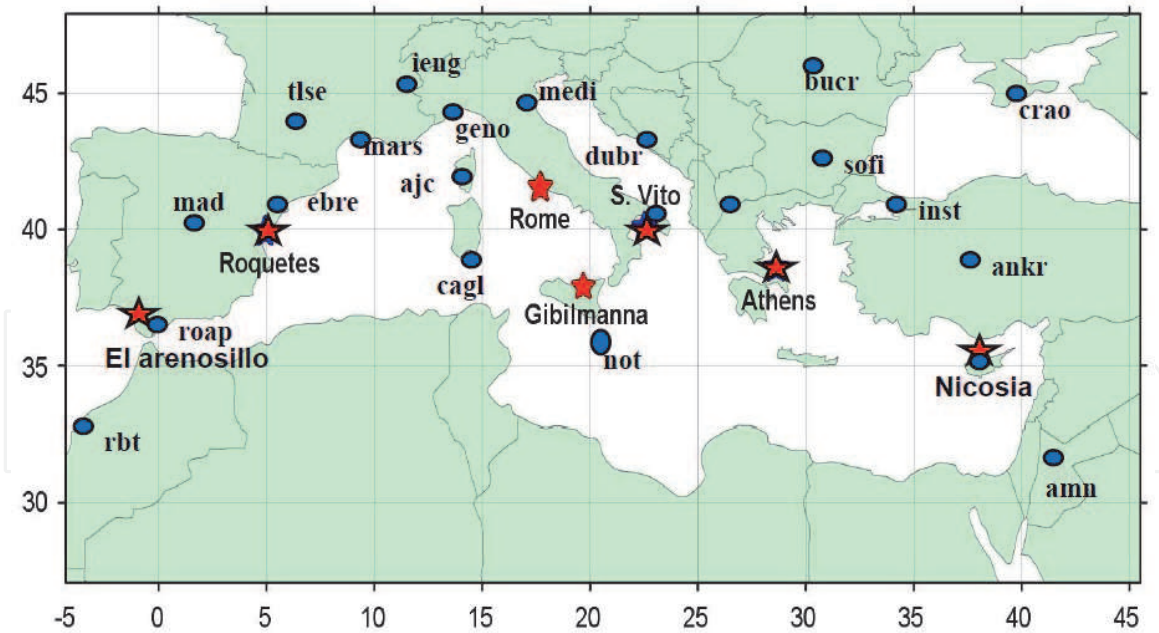
Figure 1.
Map of Mediterranean and north African regions depicting the real-time operating ionosondes (red stars) and GNSS sites (blue points). (www.igs.org/network).

true for the transition area between mid-latitude and equatorial ionosphere where the Mediterranean and North African regions have a special importance for iono-spheric studies and applications. Moreover, the sea and deserted areas in these regions make even more important ionospheric monitoring and modeling because of limited availability of sufficient and high-quality data for activities in a broad range of areas within geophysics. **Figure 1** shows the positioning of the ionosondes and GNSS receivers, as principal sources of ionospheric information within Mediterranean and North African regions, respectively.

In order to illustrate ionospheric monitoring and modeling results applicable to coastal and marine environments, Section 2 discusses in brief the salient points of the well-established physical background of the Earth's upper atmosphere. Section 3 describes the basic principle of the main techniques systematically used for monitoring the ionized layers of the Earth's upper atmosphere based on propagation effects that influence radio waves traveling through the ionosphere. Section 4 contains an overview of the current state of the most important electron density models, while particular attention is given to ionospheric mapping techniques to spatially interpolate derived parameters between sites from the sparse network of measurements and/or observations with emphasis on local and/or restricted area. Some aspects of HF communications in coastal and maritime applications are described in Section 5. Finally, Section 6 briefly summarizes the work, notes limitations of the current methodology, and suggests areas for further study.

2. General description of the Earth's ionosphere

The ionosphere is embedded in the neutral Earth's atmosphere beginning at an altitude of about 50 km and extending outward up to 1000 km. It is dynamic plasma medium, highly variable in space on scales of meters to hundreds of kilometers and time on scales of seconds to hour, months, and solar cycles that exhibit climatology and weather features at all latitudes, longitudes, and altitudes. The Earth's ionosphere is created and maintained on a very regular basis by energetic solar irradiance in the extreme ultraviolet (EUV) and X-ray regions of the spectrum that

ionizes a part of the neutral atmosphere. Absorption of EUV radiation at other wavelengths also heats a small fraction of the neutral atmosphere so that the deposition of this energy drives a complex cycle of photochemical response that interacts strongly with atmospheric transport. Solar variation of its spectrum on timescales as long as the 11-year solar activity cycle can have a significant effect on ionospheric structure and dynamics, and hence on propagation parameters, in terms of solar cycle, annual, seasonal, daily, and hourly variations [1, 2].

The maximum expansion of the ground-based ionospheric measurements was achieved during the International Geophysical Year (IGY, July 1957 to December 1958) and has steadily continued to the present days. Since 1995 the US Global Positioning System (GPS) has made possible the electron content observations along a radio signal path between a satellite and a ground receiver station, with valuable total electron content (*TEC*) data coming from sustained growth of GNSS technologies. Measured quantities like critical frequencies f_0E, f_0F1, and f_0F2 are related to ionospheric layers, the F2 layer (atomic oxygen ions) around 350 km altitude, the daytime F1 layer (molecular oxygen ions) around 190 km and E layer at 120 km, and the D layer near 70 km (**Figure 2**). Separate regions in the Earth's ionosphere including topside part above 1000 km are direct consequence of solar spectrum energy deposited at various heights depending on absorption of atmosphere, of recombination processes depending on density of atmosphere changeable with height, and of the upper atmosphere composition itself also variable with height. The various forms of temporal and spatial variability of each ionospheric layer include both systematic diurnal, seasonal, and solar cycle variations and large irregular variations. They are also a function of geomagnetic latitude as the role of the Earth's magnetic field is essential, and in solar-terrestrial physics, it is very often described by geomagnetic indices such as *Dst*, *AE*, *Kp*, and *Ap* [3].

From **Figure 2** it is clear that the F2 layer has the greatest plasma density, with maximum electron density $NmF2 = 1.24\ 10^{10}\ foF2^2$ (see also Eq. 3), which carries the highest frequencies for less absorption, and radio waves can travel the furthest distance with a minimum of attenuating hops making this ionospheric region the most important for HF communications. Its rapid changes throughout the day are shown in **Figure 3** by an example of the day-to-day *foF2* variability at the Nicosia (35.1° N, 33.3° E) ionosonde station over temporal scales from 15 minutes to 1 month
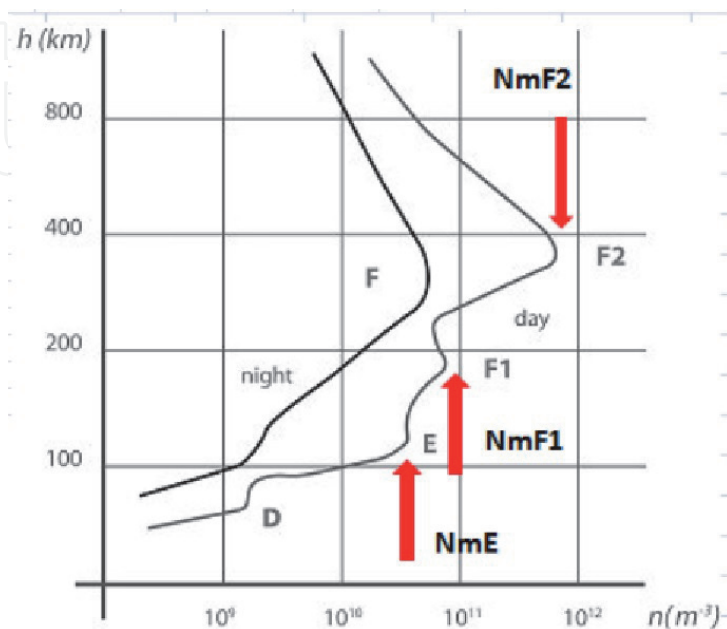

Figure 2.
Diurnal and nocturnal ionospheric N(h) profile representing electron density as a function of height.
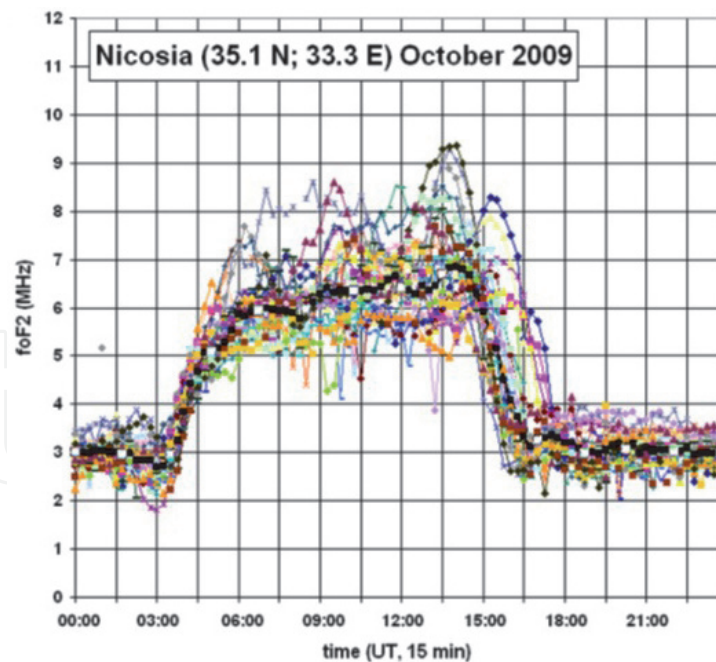
Figure 3.
Plot of the day-to-day critical frequency foF2 *variability over temporal scales from 15 minutes to 1 month at the Nicosia ionosonde station during a period of very low solar activity in October 2009 with the monthly mean of the daily sunspot number Ri = 4.6. The* foF2 *monthly median is in black.*

of October 2009, representing ionospheric equinox during very low solar activity conditions. During this particular month, overall *foF2* departure from the monthly median values is about ±30%, while during very high solar activity conditions, departure from median conditions is usually much greater following the ratio of the corresponding values of solar radio flux *F10.7*, an index derived from measurements of total emission originating from high in the solar chromosphere and lower corona thus frequently used as a very good indicator of solar activity [2].

Similar results of the high variability are obtained if the maximum ionization density is replaced by the column density or vertical total electron content, *VTEC*, of the ionosphere at the co-located GNSS station at the site nico (35.1 N, 33.4 E), in Cyprus (http://www.igs.org/). **Figure 4** shows diurnal 10 minutes *VTEC* values during absolute solar minimum in December 2008 when the variability around the monthly median values is around ±40% during the nighttime and a little lower during the daytime ≈ ± 30%. Again it has to be emphasized that solar cycle dependence is fundamental when values of *VTEC* around solar maximum largely exceed by a factor of approximately 2 for those around solar minimum.

Solar events such as flares and coronal mass ejections often produce large variations in the corpuscular and electromagnetic radiations leading to disturbances of the regular regions known as ionospheric storms. They have important terrestrial consequences generating large disturbances in ionospheric electron density distribution $N(h)$, total electron content *TEC*, and the electric currents system. All these phenomena can continue for a few hours to several days and lead to significant changes in the ionospheric plasma parameters which can be particularly damaging to both satellite- and ground-based systems. The F region's response to ionospheric storms has been studied since the earliest days of solar-terrestrial physics more than 90 years ago. In general results show consistency in characteristic patterns of an ionospheric storm: (1) a short positive phase that occurs during the daytime hours on the first day of a storm with the tendency to significantly increase electron density during the first 24 hours of the storm above its quiet time reference level and (2) a prolonged negative phase on subsequent days leaning to significantly
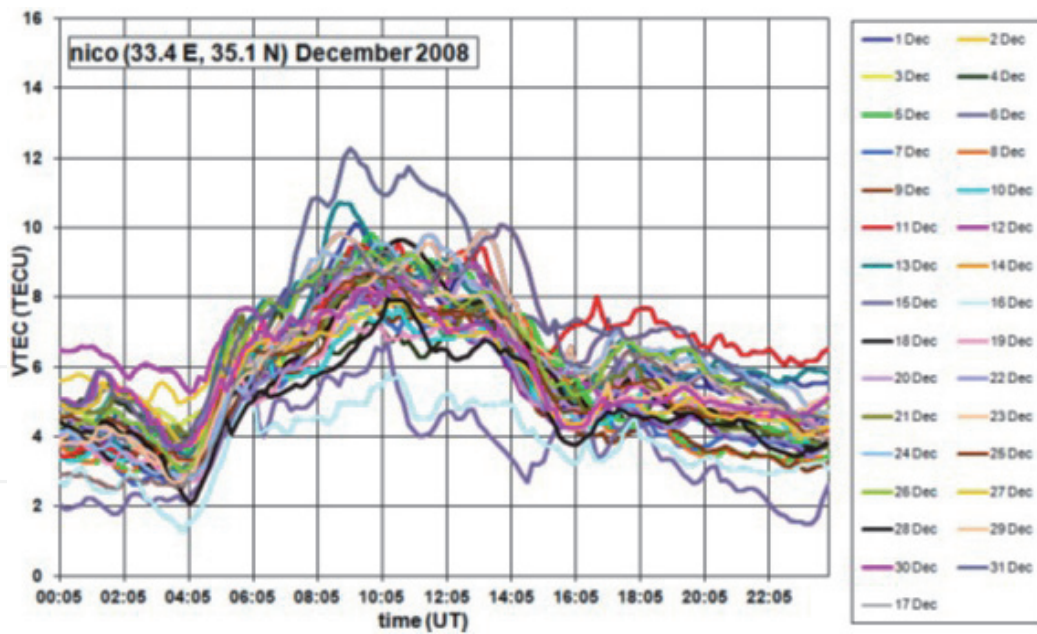
Figure 4.
Plot of the day-to-day vertical total electron content VTEC variability at the nico GNSS station over temporal scales from 10 minutes to 1 month during absolute solar minimum in December 2008 with the monthly mean of the daily sunspot number Ri = 0.8.

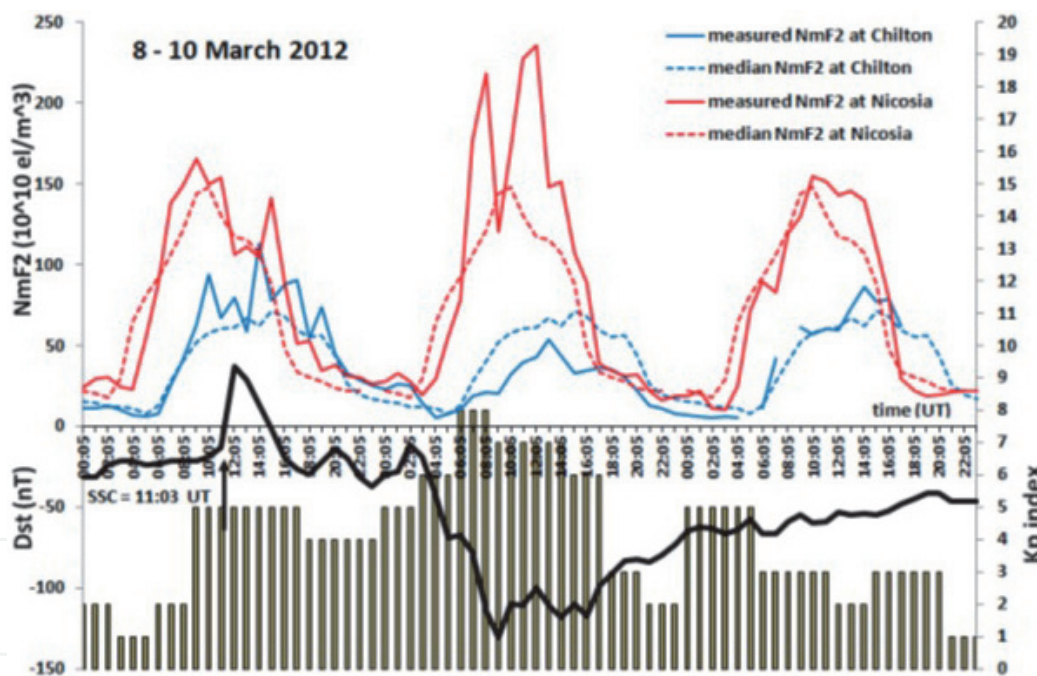
Figure 5.
Time variations in Dst and Kp geomagnetic indices and NmF2 at the Chilton (51.6° N, 358.7° E) (blue solid and dashed curves) and at Nicosia (35.1° N, 33.3° E) ionosonde stations (red solid and dashed curves) during the ionospheric storm period of 8 –10 March 2012.

decrease electron density below its quiet time reference level, with recovery in 1 or 2 days later [see solid and dashed blue curves for the high mid-latitude Chilton (51.6° N, 358.7° E) ionosonde station in **Figure 5**].

Remarkable differences occur in the magnitudes and longevities of the only positive storm pattern represented with solid and dashed red curves for the low mid-latitude Nicosia (35.1° N, 33.3° E) ionosonde station at the island of Cyprus in the Mediterranean Sea. The striking feature is the pronounced *NmF2* increase above monthly median values, which has been taken to represent the quiet reference level at both stations. It is to be believed that short-timescale dynamical mechanisms

driving the storms (electrodynamical and thermospheric) dominate the positive phase, while longer-timescale composition changes the negative phase [4, 5].

However a number of questions remain, e.g., solar-terrestrial circumstances and prior storm ionospheric condition necessary for these phases to occur. In particular: (1) duration and magnitude of the negative and/or positive phase versus latitude, local time, season, and phase of solar cycle as well as between different solar cycles and (2) temporal relationships between characteristics of the solar event and the consequent development of the geomagnetic and ionospheric storms in real time. Nowadays they are subjects of intense studies within the space weather domain [2].

3. Ionospheric monitoring

The exploration and the physical description of the ionosphere has been the result of a great activity of experimental observation and continuous systematic monitoring started at beginning of the last century when, G. Marconi realizing on 12 December 1901 a transoceanic radio link, provided the experimental proof of the existence of the Earth's ionosphere postulated during the nineteenth century by various scientists like B. Stewart and A. Schuster. Then the vertical structure of this part of the atmosphere has been described in detail thanks to the technological developments of G. Breit and M. A. Tuve and to the systematic experiments and theoretical studies of Appleton [6].

Two principal methods have been applied to observe and to investigate the terrestrial ionosphere: the first and traditional one is ground-based, the ionospheric vertical sounding by ionosondes to determine electron density of ionospheric plasma as a function of the height, and the second one, more recently, by using geostationary satellites to provide the total electron content.

The first one is a special radar technique based on the principle that when an electromagnetic wave of frequency f penetrates vertically in the ionospheric plasma, the reflection occurs, according to the magneto-ionic theory [7], at the level where the refractive n index becomes zero:

$$n^2 = 1 - \left(f_N/f \right)^2 \tag{1}$$

Then considering that the plasma frequency f_N is

$$f_N = \left[\left(Nq^{2)} \right) / \left(4m\pi^2 \varepsilon_0 \right) \right] \tag{2}$$

where N is electron density and q and m are the charge and the mass of the electron, respectively; the reflection in the ionosphere occurs when the incident frequency f is equal to f_N. Furthermore the maximum electron density Nm corresponds to the maximum reflected incidence frequency, called the critical frequency fo:

$$Nm = 1.24 \ 10^{10} \ fo^2 \tag{3}$$

where Nm and fo are expressed in el/m^3 and in MHz, respectively.

A vertical ionospheric sounder emits radio impulses with increasing frequency from 1 to 20 MHz, measuring the time delay of radio signals received back from the different ionospheric layer:

$$\Delta t = 2 \ h'/c \tag{4}$$

the function of the virtual height of reflection *h'* is virtual because the signal travels more slowly in the ionosphere than in the free space so that the observed heights *h'* exceed the true height reflections.

The ionogram, the record produced by the ionosonde, is a plot of the virtual height of reflection vs. the transmitted frequency. In **Figure 6** a typical ionogram is shown produced by a modern digital ionosonde [8], where several important characteristics (like the critical frequencies and the heights of the different ionospheric layers) are indicated as well as the automatic interpretation on the left side. They all have a significant role in the studies concerning ionospheric physics, space weather, and related phenomena.

The routine observations of every ionospheric station need standard techniques and conventions applicable for the interpretation of ionospheric measurements in order to achieve a more phenomenological description of the ionogram as well as provide a simplified description of the ionosphere above the station. They were defined in the URSI handbook of ionogram interpretation and reduction edited by W.R. Piggot and K. Rawer [9]. During the past decades, the ionosondes have had an important technological evolution from the first ones analogical recorded on film, to the digital one, and more recently is the automatic scaling of the ionograms essential for real-time monitoring the ionospheric plasma of space weather purposes [1, 2].

The other principal method of ionospheric observation, the GNSS signals monitoring, is applied to evaluate the ionospheric total electron content, *TEC*, defined as the integral of electron density along the radio wave path s from a satellite transmitter to a ground-based receiver:

$$TEC = \int_s Ne(s)\, ds \tag{5}$$

where *Ne* is the ionospheric electron density along the path *s* in electrons/m^3.

This parameter providing information of overall ionization in the ionosphere-plasmasphere system is particularly important for trans-ionospheric communications (propagation at VHF and above), navigation, and solar-terrestrial physics. Considering that the satellite is not at the zenith point of the receiver
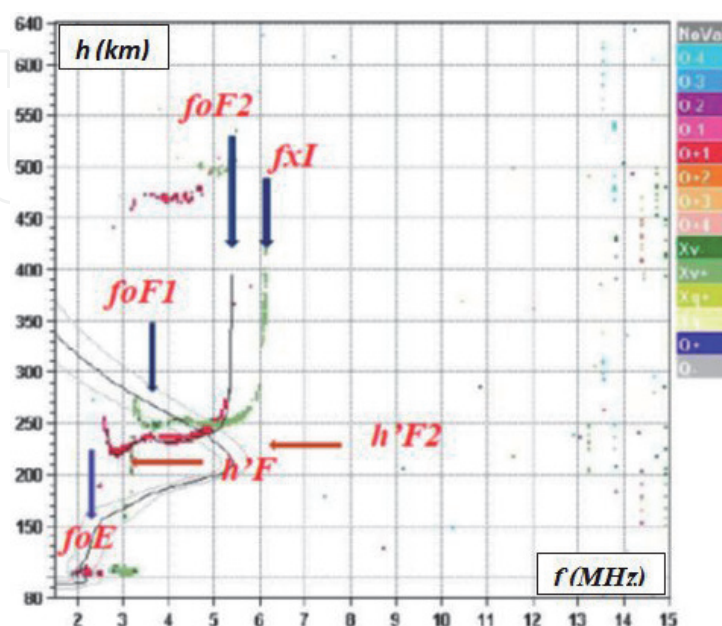

Figure 6.
Daytime ionogram produced by a digisonde, a digital ionosonde, with routinely scaled ionospheric characteristics.

and the real path s is not vertical, it is possible to calculate the vertical *TEC* (*VTEC*) by using different geophysical models to convert the values of the so-called slant *TEC*.

The technique to evaluate the *TEC* is based on the physical fact that the signal propagation time between the satellite- and the ground-based receiver, due to the anisotropic nature of the ionosphere-plasmasphere system, is directly proportional to the total number of free electrons along the signal path. The great increase and technological development on the satellite navigation and positioning system provided a new source of ionospheric data available at several global and regional centers of the International GNSS Service formerly the International GPS Service for Geodynamics (IGS) (http://igscb.jpl.nasa.gov/) in the receiver independent exchange (RINEX) format [10]. These observations are particularly important in the evaluation of the error due to the ionospheric propagation delay for the single GNSS frequency that is inversely proportional to the square of its carrier frequency but proportional to *TEC* along the ray path. The Center for Orbit Determination in Europe (CODE) from Universität Bern (http://aiuws.unibe/ch/ionosphere) regularly provides global *VTEC* maps, while the International GNSS Service makes available an extensive variety of GNSS open data and ionospheric open products (http://www.igs.org/).

4. Ionospheric modeling and mapping

The ground-based and satellite routine measurements constituted, in the second half of last the century, the basis for the global, regional, and local modeling of the terrestrial ionospheric plasma. This activity was supported by international organizations, like the International Union of Radio Science (URSI), the Committee on Space Research (COSPAR), and in particular the International Radio Consultative Committee (CCIR) establishing internationally agreed global propagation models.

Simple models of the lower layers E and F1 are defined as Chapman layers, because referred to an ideal ionosphere as function of the solar zenith angle χ, then the geographical position, and of a solar activity index R [11]:

$$foE\,(\chi,R) = 3.3\,[(1+0.0088R)\ cos\ \chi]^{1/4} \tag{6}$$

$$foF1\,(\chi,R) = 4.25[(1+0.015R)\ cos\ \chi]^{1/4} \tag{7}$$

where *foE* and *foF1* are the critical frequencies in MHz.

However, essential for theoretical studies and practical application are 3D pictures of the terrestrial ionosphere generated by combining the models of the electron density profile, the concentration of the electrons vs. the altitude (see **Figure 2**), and the global and regional mapping of the principal ionospheric characteristics. After the well-known and widely used model introduced by P.A. Bradley and J. Dudney [1], important results were obtained by more general empirical International Reference Ionosphere (IRI) model [12]. Following the beginning of IRI project in 1968, this global model has been systematically improved and updated over time, so that it is currently accepted as the standard for ionospheric parameters in the altitude range from 60 to 2000 km.

Thanks to the first use of computing devices, able to manage the enormous amount of observations collected during the years around the IGY, a numerical method was developed in the Institute of Telecommunication Sciences (ITS) at the Boulder Laboratories of the U.S. Department of Commerce by W.B. Jones and R.M.

Gallet [13] to produce global maps of the two key ionospheric characteristics related to the maximum electron density of the ionospheric F region. They are the median monthly hourly values of *foF2* and *M(3000)F2*, obtained from ionograms of the worldwide ionosonde network. These maps are extremely important for long-distance HF communications representing a significant tool for applied science and for radio users, especially frequency planners at radio broadcasting agencies as well as for geophysicists of the upper atmosphere. Here *M(3000)F2* is the transmission *M* factor (also known as the propagation, obliquity, or maximum usable frequency (*MUF*) factor), an ionospheric characteristic derived from an empirical estimate of the relationship between reflecting layer height, frequency, and oblique radio wave propagation path length [9]. The other important propagation and prediction quantity is the maximum usable frequency, a function of a critical frequency *fo* and an appropriate *M* factor for a given distance *d*:

$$MUF\ (d) = fo\ M\ (d) \tag{8}$$

To produce regional models of the ionosphere for long-term prediction, nowcasting or even short-term forecasting with accuracy much better of the global mode was the target of European projects promoted by the European scientific framework, European Cooperation in Science and Technology (COST) [14]. In **Figure 7** an example of the hourly foF2 nowcast map is given generated by using simplified ionospheric regional model real-time updated (SIRMUP) model for the digital upper atmosphere server (DIAS) [15], an application also embodied in the project ESPAS, the near-Earth space data infrastructure for e-Science (https://www.espas-fp7.eu/).
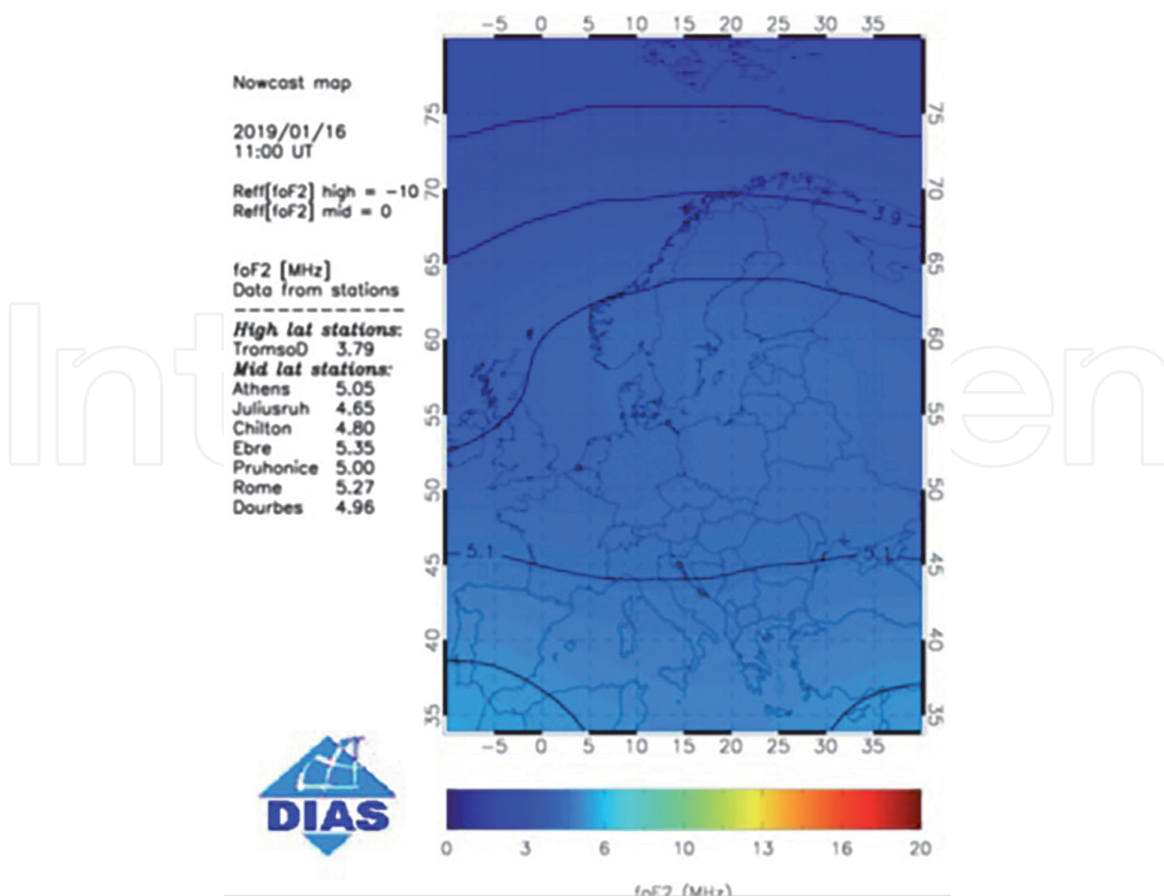

Figure 7.
An example of the foF2 *nowcast map predicted by SIRMUP model in 16 January 2019 at 11:00 UT for DIAS (http://www.iono.noa.gr/Dias/).*

5. HF communications in coastal and maritime applications

HF radio links via ionospere in the 3–30 MHz band represented in most part of the twentieth century the only way for long-distance radio communications, largely used by military and civilian users. Consequently the scientific research in ionospheric radio propagation and monitoring was mainly supported by those countries having global interests and among them the air and maritime communications [16]. The new and great increase of satellite use for long-distance communications gave, between the end of the 1970s and the beginning of the 1980s, the impression that the HF radio communication via ionosphere should be rapidly obsolete. Instead, the use of HF still plays a very important role during emergency situation as the natural catastrophes, for naval or coast to island communications, for people sparse in large extension of country, and for military and civilian radio links located in valleys of a mountain region. So the prediction, forecasting, or even the nowcasting of the future status of the reflectivity of the ionospheric layers is crucial for radio planners to choose the best radio frequency to use or, more recently to know, the evolution of the overall space weather conditions [2].

In a typical HF radio link via ionosphere (**Figure 8**), radio users need to know in advance the range of the useful radio frequencies to be applicable for their service and the area covered by them. The spectrum of the radio frequencies between two points is included between the maximum usable frequency and the lower usable frequency (*LUF*). The *MUF* depends only on the geometry of the radio link and on the conditions of reflectivity of the ionosphere, practically the critical frequency *fo* of the ionospheric layer, while the *LUF* depends, besides geophysical parameters
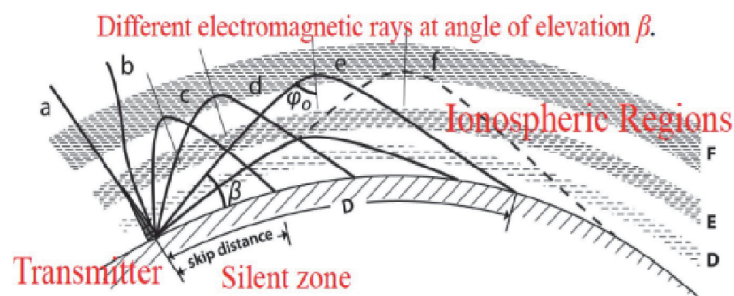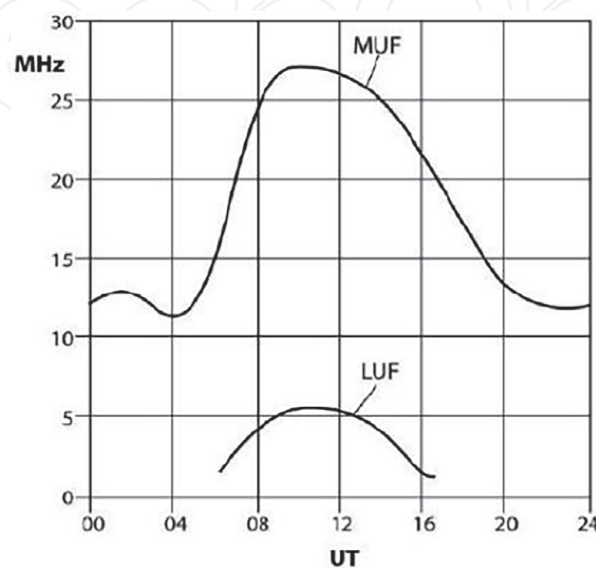

Figure 8.
Simple scheme of an ionospheric radio link.

Figure 9.
Example of the HF ionospheric long-term prediction of MUF *and* LUF *for a point-to-point radio link.*

and geometry, principally on the radio technical characteristics of the equipment like power of the transmitter, sensitivity of the receiver, radio noise, gain of the antenna system, etc. [1, 11].

Different national and international institutions provide long-term prediction of the hourly behavior of *MUF* and *LUF* for a given radio link. See as an important example the many radio and space weather information provided by the Australian SWS-Radio and Space Services at https://www.sws.bom.gov.au/, the American NOAA with the IONCAP procedure at ftp.ngdc.noaa.gov/STP/IONOSPHERE/ MODELS/IONCAP/, the France Telecom at www.iono.enst-bretagne.fr, and the already mentioned DIAS/ESPAS services. Other national institutions also provide ionospheric prediction, for example, the Italian INGV (Istituto Nazionale di Geofisica e Vulcanologia), inside European organizations or by special request of
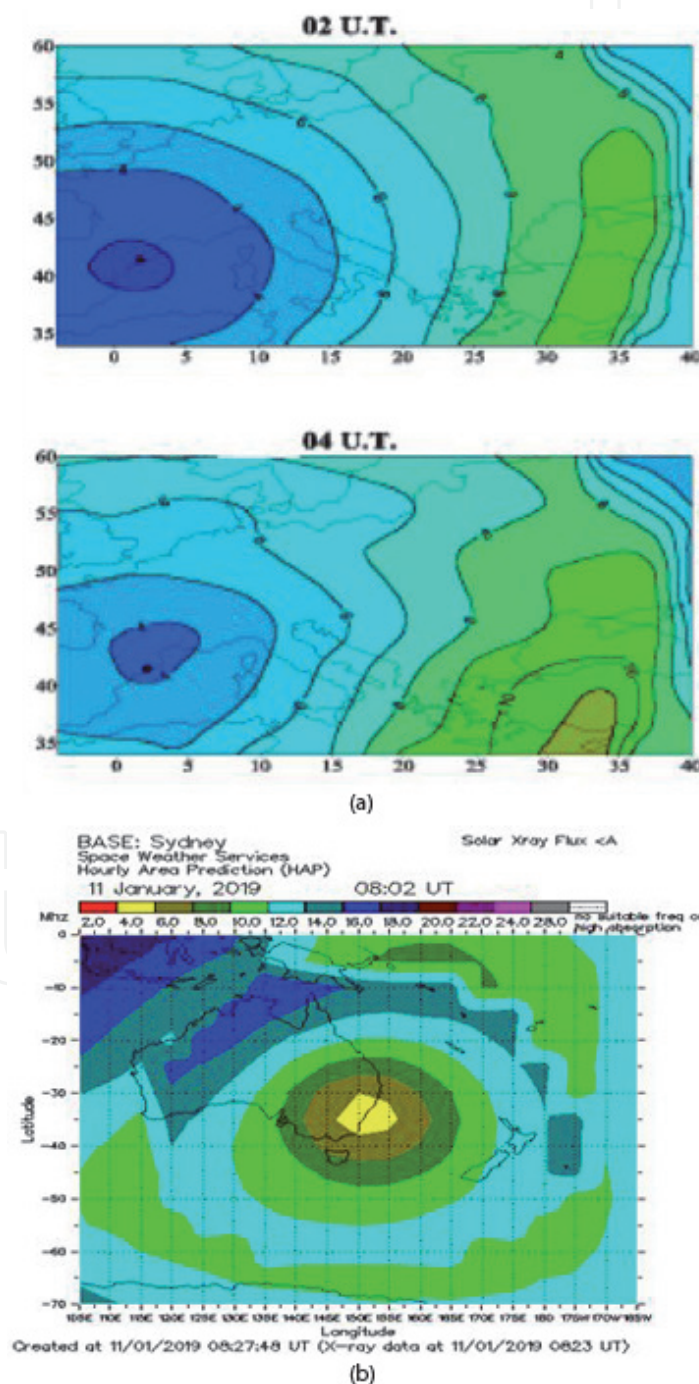

Figure 10.
Skip distance maps or MUF isolines in two typical examples provided by national services: (a) applied to the Mediterranean area and (b) applied to the Australian region provided by the Australian radio and space services at https://www.sws.bom.gov.au › HF_Systems.

their users. For example, in **Figure 9** a schematic pattern of the *MUF* and *LUF* hourly monthly median predictions for a generic distance and month is shown.

Another parameter extremely relevant to the class of users like the broadcasting agencies and air and maritime application is the skip distance, defined as the minimum distance reflected from the ionosphere, drawn by isolines around the transmitting point. This parameter, typical for radio links from a fixed point to a mobile receiver, is derived by the *MUF* and gives information on the area covered by a given frequency; in fact within this distance, also known as the silent distance, only ground wave propagation is possible.

In **Figure 10** there are two examples of this kind of service. The first one, on the upper panel, applied to the Mediterranean area, gives the hourly isolines of the *MUF* in MHz or the skip distance variable with time for a point of transmission located in South East. This sequence of maps clearly shows the effect of the Sun,
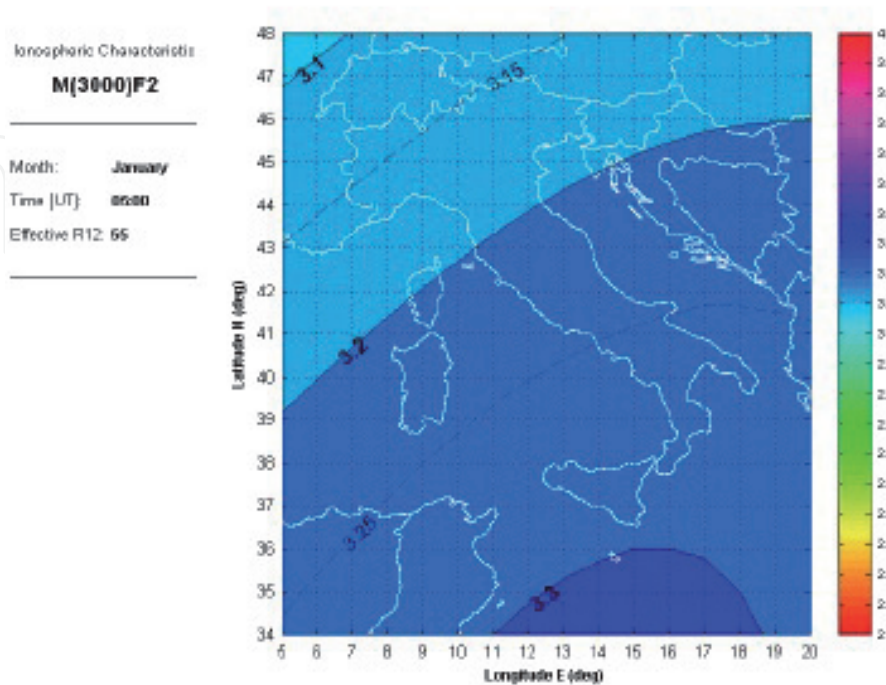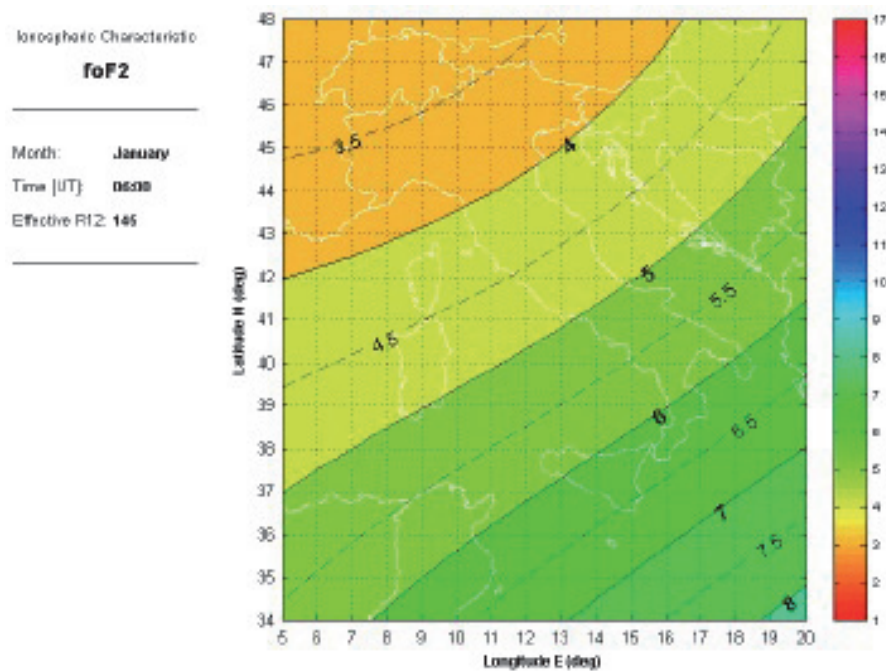

Figure 11.
Examples of foF2 *and* M(3000)F2 *nowcast maps predicted by SIRMUP model for the Central Mediterranean area at two different hours and effective solar activity index $R_{12}eff$.*

increasing the electron density from the South East. The second one, on the lower panel, provided by the Australian Radio and Space Services gives the nowcast optimum recommended frequency for the Australia region and the close-up oceans having a transmitter located at Sydney (http://www.sws.born.gov.au › HF_Systems).

Of course the first and most important application of the ionospheric radio propagation in the coastal and maritime communication is related to the point-to-point radio links between the country and the islands establishing a continued contact between the government critical infrastructures when they are not covered, due to the distance, by other options like VHF radio bridges or ground wave propagation. Secondly, HF radio communication is obviously still important for constant communication of civilian radio users, i.e., the small boats of fishermen and even for the national Coast Guard boats, especially in the Mediterranean area where there are recent operating rescue actions far from their country coast. The Mediterranean area is particularly interesting for the ionospheric physics and radio propagation, not only for historical, economical, and political reasons, but also because in that area, there are the southernmost systematic ionospheric soundings when no other ionospheric observations are available in all the northern part of the African region.

In **Figure 11** two nowcasting maps of *foF2* and *M(3000)F2* are shown produced by the Geomagnetic Indices Forecasting and Ionospheric Nowcasting Tools
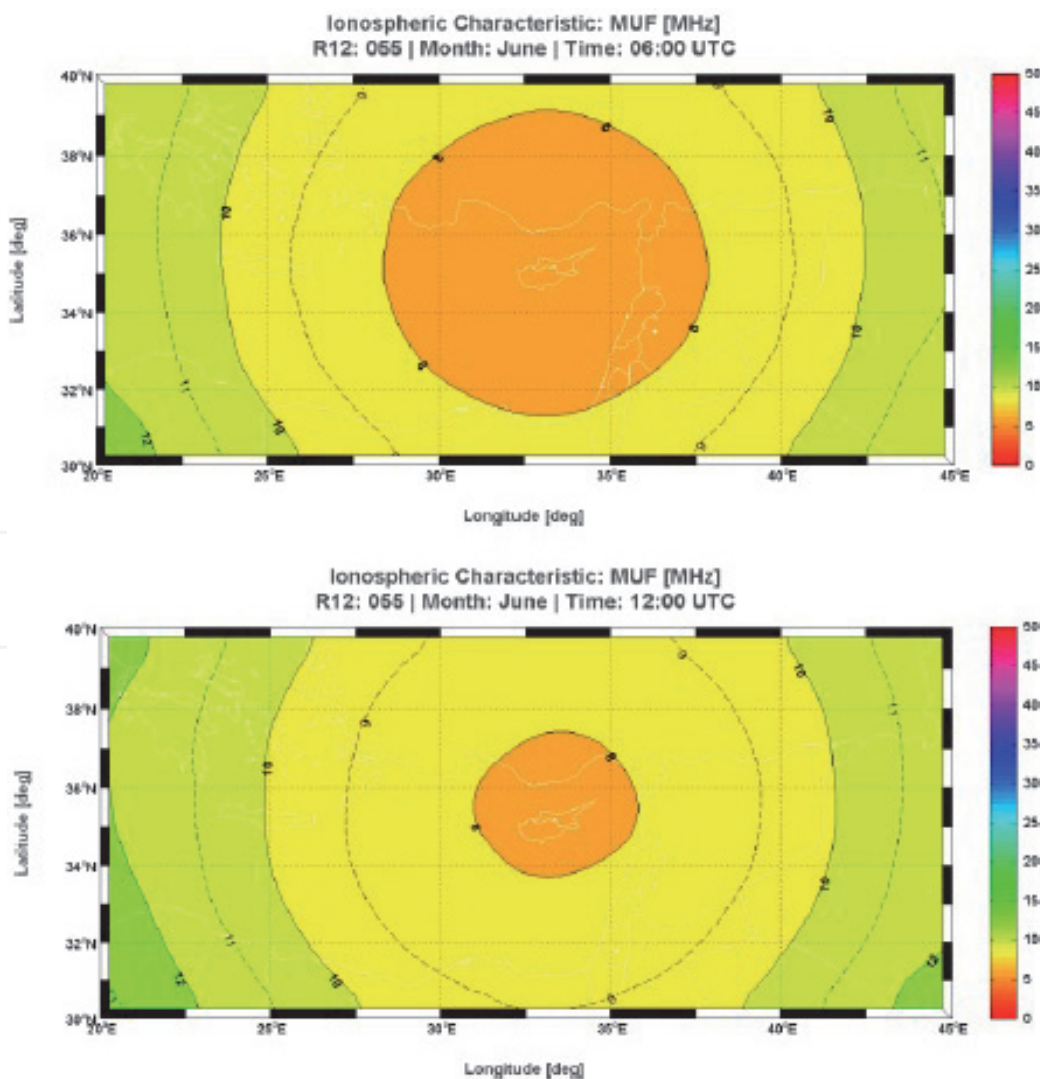

Figure 12.
Example of long-term maps of MUF *over the eastern part of the Mediterranean Sea predicted by SIRM for the Cyprus Ionospheric forecasting service.*

(GIFINT) [17], one of the space weather pilot projects promoted by the European Space Agency in the central area of the Mediterranean Sea.

Long-term maps of the *MUF* in the Eastern part of the Mediterranean area are available within the Cyprus Ionospheric Forecasting Service (CIFS) [18] project promoted by the Frederick Research Center of Nicosia, Cyprus, in **Figure 12**.

The technique involved in the over-the-horizon (OTH) ionospheric radar (**Figure 13**) uses HF frequencies reflected by the ionosphere to detect objects at very long distances, not covered by the ordinary radars that cannot operate beyond the horizon [19, 20]. This technique needs a very high level of energy transmitted (from hundreds of MWatt to GWatt) and a large and complex structure of the antenna system (hundreds of square meters). A real-time control of the ionosphere by a network of ionospheric vertical soundings together with the 3D image and the ray tracing model of the ionosphere is also necessary. **Figure 14** gives an example of 3D image of the ionosphere in the Mediterranean region applicable accordingly [21].

The OTH ionospheric radar, besides the obvious military use, has two important applications from the point of view of the coastal environment. The first one is the control of naval traffic in the space around the territorial waters in other words the border control. The second one is the remote control of the status of the sea level in order to detect tsunami waves for an early alert [22].

Finally, another important application of the HF ionospheric communication has been described within objectives of the European project Short Wave Critical Infrastructure Network based on New Generation (SWING) of high survival radio communications system [23]. The SWING project performed a study to maintain a high survival HF radio network (data/voice) in the real-time support of European critical infrastructure communications. This operating activity should establish a minimum flux of essential information for the management and control, in case, of
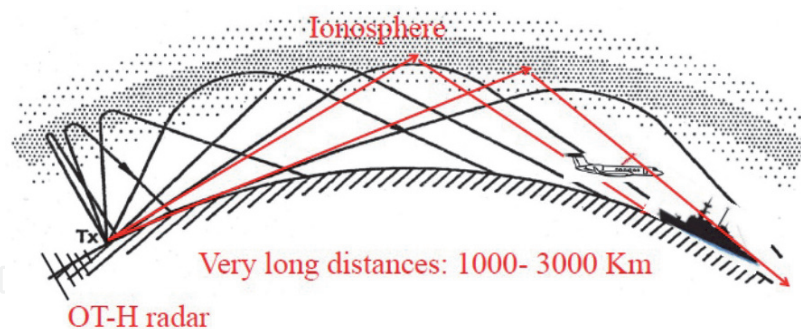

Figure 13.
Simple scheme of the OTH operation for long-range detection of ships, aeroplanes and sea surface conditions.
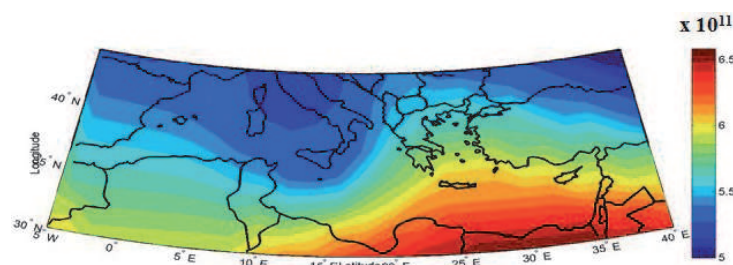

Figure 14.
Map of the ionospheric electron density in el/m³ at the fixed height of 201 km obtained by the IRI-SIRMUP-P procedure for a given epoch.

wide scale of natural disasters or cyberattacks to render Internet links useless between the great islands of the Mediterranean region and their respective government organization.

6. Conclusions

The land and maritime mobile community for communication of voice and data, in coast stations, ship-ship, shore-ship, and ship-shore modes of operation, occupied about 15% of available HF radio spectrum. High-frequency transmissions and prediction support both maritime safety information (MSI) and distress related communications using digital selective calling (DSC). These communications take place across the maritime mobile service bands within 1.6–26.5 MHz as defined by the International Telecommunication Union (ITU) Radio Regulations [24]. More importantly there is currently considerable worldwide effort being applied to further expand the use of GNSSs by civilian users in general and the civil aviation community in particular. This effort is being directed toward switching from systems under military control to systems under civil control. Scientific studies and technical reports have supported a variety of work in these areas, but here focus is on the Earth's ionosphere's important role. One of the main reasons is related to the fact that this ionosphere is a medium of communication inexhaustible, not polluting and extremely economic especially for its role of possible backup in case of blackout of other systems.

However, the highly complex nature of the Earth's ionosphere, and its potential for huge spatial and temporal variability, is such that a very large number of modeling scenarios is required in general and coastal and marine environments in particular. It has been briefly shown that the algorithms used in this study can be tuned and optimized so as to meet the basic requirements, even under the worst-case space weather conditions [25]. The SIRM, and its real-time updating version SIRMUP, provides regional type of a self-consistent model initialization specifying most important ionospheric characteristics *foF2* and *M(3000)F2* at a given time, while the GIFINT approach could assess specifications and forecasts of ionospheric variables on a local level. This further enhances the necessity for a large number of varied scenarios to be used for verification purposes.

Problems of data shortage, within the Mediterranean and North African regions, and a potential lack in confidence in the performance of models based on such limited data sets have taken on greater importance in recent years. As real-time system operations and integrated management are becoming increasingly present in many domains within geophysics, which requires an increased amount of data with high spatiotemporal resolution, synthetic data is required to augment recorded data and to ensure that a wide variety of ionospheric conditions are tested and an associated model is verified.

Geomagnetism, Kyoto, for the production of Ds index (http://wdc.kugi.kyoto-u.ac.jp/); and the International GNSS Service (IGS) for providing GNSS open data (http://www.igs.org/).

Conflict of interest

None.

Author details

Ljiljana R. Cander[1]* and Bruno Zolesi[2]

1 Rutherford Appleton Laboratory, Harwell Oxford, UK

2 Istituto Nazionale di Geofisica e Vulcanologia, Rome, Italy

*Address all correspondence to: ljiljana.cander@stfc.ac.uk

IntechOpen

References

[1] Zolesi B, LjR C. Ionospheric Prediction and Forecasting. Heidelberg, New York, Dordrecht, London: Springer; 2014

[2] LjR C. Ionospheric space weather. In: Springer Geophysics. Cham, Switzerland: Springer Nature Switzerland AG; 2019

[3] Lanza R, Meloni A. The Earth's Magnetism, an Introduction for Geologists. Heidelberg: Springer-Verlaig; 2006

[4] Prölss GW. Physics of the Earth's Space Environment: An Introduction. Berlin, Heidelberg: Springer; 2004

[5] Mendillo M. Storms in the ionosphere: Patterns and processes for total electron content. Reviews of Geophysics. 2006;**44**. DOI: 10.1029/2005RG000193

[6] Appleton EV. Some notes on wireless methods of investigating the electrical structure of the upper atmosphere. I. Proceedings of the Physical Society. 1928;**41**:43-59

[7] Ractliffe JA. The Magneto-Ionic Theory and its Applications to the Ionosphere. Cambridge: Cambridge University Press; 1962

[8] Reinisch BW, Huang X. Automatic calculation of electron density profiles from digital ionograms 3, processing of bottomside ionograms. Radio Science. 1983;**18**:477-492

[9] Piggot WR, Rawer K. U.R.S.I Handbook of Ionogram Interpretation and Reduction. World Data Center a for Solar Terrestrial Physics-Report UAG-23. Asheville: NOAA, Environmental Data Service; 1972

[10] Dow JM, Neilan RE, Rizos C. The international GNSS service in a changing landscape of global navigation satellite systems. Journal of Geodesy. 2009;**83**:191-198. DOI: 10.1007/s00190-008-0300-3

[11] Davies K. Ionospheric Radio. IEE Electromagnetic Waves Series 31. London: Peter Peregrinus Ltd; 1990

[12] Bilitza D. International reference ionosphere 2000. Radio Science. 2001;**36**:261-275

[13] Jones WB, Gallet RM. Ionospheric mapping by numerical methods. Telecommunication Journal. 1960;**12**:260-264

[14] Zolesi B, LjR C. The role of COST actions in unifying the European ionospheric community in the transition between the two millennia. History of Geo- and Space Sciences. 2018;**9**:65-77. DOI: 10.5194/hgss-9-65-2018

[15] Zolesi B, Belehaki A, Tsagouri I, LjR C. Real-time updating of the simplified Ionospheric regional model for operational applications. Radio Science. 2004. DOI: 10.1029/2003RS002936

[16] Anduaga A. Wireless & Empire. Oxford: Oxford University Press; 2009

[17] Pallocchia G, Bertello I, Amata E, Consolini G, Pezzopane M, Zolesi B, et al. The GIFINT Space Weather products. Conference paper, First European Space Weather Week, Noordwijk; 2004

[18] Pezzopane M, Zolesi B, Pietrella M, Haralambous H, Oikonomou C, Cander LjR. Ionospheric Prediction and Forecasting Services in Mediterranean Area. Conference paper, General Assembly of the European Geophysical Union, Wien, April 2014

[19] Reinisch BW, Haines DM, Bibl K, Galkin I, Huang X, Kitrosser DF, et al.

Ionospheric sounding in support of over-the-horizon radar. Radio Science. 1997;**32**(4):1681-1694

[20] Francis DB, Cervera MA, Frazer G. Performance prediction for design of a network of sky wave over-the-horizon radars. IEEE Aerospace and Electronic Systems Magazine; 2017;**32**(12):18-28. DOI: 10.1109/MAES.2017.170056

[21] Pezzopane M, Pietrella M, Pignatelli A, Zolesi B, Cander LR. Assimilation of autoscaled data and regional and local ionospheric models as input sources for real time 3D international reference ionosphere modeling. Radio Science. 2011;**46**. DOI: 10.1029/2011RS004697

[22] Artru J, Lognonné P, Occhipinti G, Crespon F, Garcia R, Jeason E, et al. Tsunamis detection in the ionosphere. Space Research Today. 2005;**163**:23-27

[23] Zolesi B, Bianchi C, Meloni A, Baskaradas JA, Belehaki A, Altadill D, et al. "SWING": A European project for a new application of an ionospheric network. Radio Science. 2016. DOI: 10.1002/2016RS006037

[24] The Radio Regulations as adopted by the World Radiocommunication Conference (WRC-15, Geneva), Edition of 2016

[25] Lanzerotti LJ. Space weather: Historical and contemporary perspectives. Space Science Reviews. 2017;**212**:1253-1270. DOI: 10.1007/s11214-017-0408-y